4-2020

Symmetry Versus Balance in Balancing Networks for Dipolar Antennas

James McLean

Heinrich D. Foltz
The University of Texas Rio Grande Valley, heinrich.foltz@utrgv.edu

Recommended Citation

J. S. McLean and H. D. Foltz, "Symmetry Versus Balance in Balancing Networks for Dipolar Antennas," in IEEE Transactions on Electromagnetic Compatibility, vol. 62, no. 4, pp. 1406-1418, Aug. 2020, doi: 10.1109/TEMC.2020.2978445.

Symmetry vs. Balance in Balancing Networks for Dipolar Antennas

James McLean[1] and Heinrich Foltz[2]

[1] *TDK R&D Corp.*
Cedar Park, TX, USA
jmclean@tdkrf.com

[2] *University of Texas Rio Grande Valley*
Edinburg, TX, USA
heinrich.foltz@utrgv.edu

***Abstract*—Imperfect balancing networks (baluns) have been identified as a source of error in emission and site attenuation measurements. For this reason performance tests have been developed to characterize the symmetry of baluns. We draw a distinction between symmetry and balance as they relate to baluns and describe both quantitatively in terms of 3-port network parameters. It is shown that a symmetric balun alone does not necessarily eliminate common-mode (CM) current on the feed transmission line. Common-mode current on the feed transmission line is minimized by use of a current balun. However, for a given implementation such as a transmission-line transformer, some types of baluns are more difficult to implement than others and an imperfect, asymmetric current balun may perform worse than another type of balun (e.g. voltage) which is more symmetric. The case of a vertically-polarized biconical antenna situated over a ground plane and driven from a coaxial feed line via a balun is examined for three symmetric baluns: a voltage balun, a current balun, and a 180° power divider. It is shown that although all three baluns are symmetric, only the current balun maintains the dipolar pattern under the asymmetrical influence of the ground plane.**

***Index Terms*—Balancing network (balun), antenna symmetry, site attenuation (SA), biconical antenna, dipole antenna, hybrid**

I. Introduction

This paper is an extended version of a paper presented at the 2019 IEEE International Symposium on Electromagnetic Compatibility in New Orleans [1]. Several contemporary standards for electromagnetic compatibility call for symmetry tests on dipolar antennas driven from coaxial transmission line via balancing networks (baluns) such as biconical antennas and tuned dipoles [2]–[4]. Both of the ANSI- and CISPR-mandated tests call for an antenna-to-antenna transmission or insertion loss measurement to be made over an open area test site (OATS) between the antenna under test (AUT) and (usually) a known-good reference antenna with the two antennas in vertical polarization as shown in Fig. 1. In these tests the AUT is typically the receive antenna. The measurement is then repeated with the AUT inverted (rotated 180° about its bore-sight axis) and the two sets of insertion loss data are compared. Scanning is sometimes employed in order to avoid errors caused by a null in the transmission due to destructive interference between the line-of-sight (LOS) and ground-bounce rays [2], [5]. Symmetry problems with baluns for vertically-polarized measurements on OATS were first noticed by M. J. Alexander and this approach for symmetry testing was originally developed at NPL [6]–[9].

This paper is for the Special Section and is an expanded version from the 2019 IEEE International Symposium on EMC and SIPI in New Orleans

The purpose of this paper is to address the operation of the balun as it pertains to symmetry and to draw a distinction between balance and symmetry. Strictly speaking, it is anti-symmetry that is required. If phase sensitive detection is employed the ideally anti-symmetric antenna/balun combination would provide identical insertion loss when inverted but 180° difference in insertion phase. Nevertheless, we will use the term symmetry here as the interpretation seems clear. As will be seen a symmetric balun does not necessarily eliminate CM current on the feed transmission line. We note that in order for the two sets of insertion loss data to be identical, it is only necessary that the balun (which is inverted) is symmetric. This is still true even if phase sensitive detection is used. That is, current balance is not requisite for the two sets of insertion loss data to be identical and for the insertion phase to change by 180° when the AUT is inverted. Therefore, we seek to concretely define the term "symmetric" as it applies to baluns.

As has been noted, a symmetric or dipolar antenna driven from a coaxial feed transmission line and operated over a ground plane can, in some cases, be rigorously represented by a 3-terminal, 2-port network [10]. This is particularly true when the balun is a shielded 3-port and the physical location of these terminals can be taken as shown in Fig. 2 so that the terminals and ports satisfy the rigorous definitions of such [11]. The 3-terminal, 2-port load representing the antenna and the exterior of balun and feed transmission line can then take the form of a T/Y or Π/Δ network as shown in Fig. 3. As is noted and supported with measurements in ref. [10], this 3-terminal representation is asymmetric in the case of a vertical dipole over a ground plane. That is, in Fig. 3 $Y_A \neq Y_C$ and $Z_A \neq Z_C$. Only a true current balun will drive or force balanced currents in this asymmetric situation. This approach might be less than satisfying, but what can be stated with some assurance is that a 2-terminal, isolated

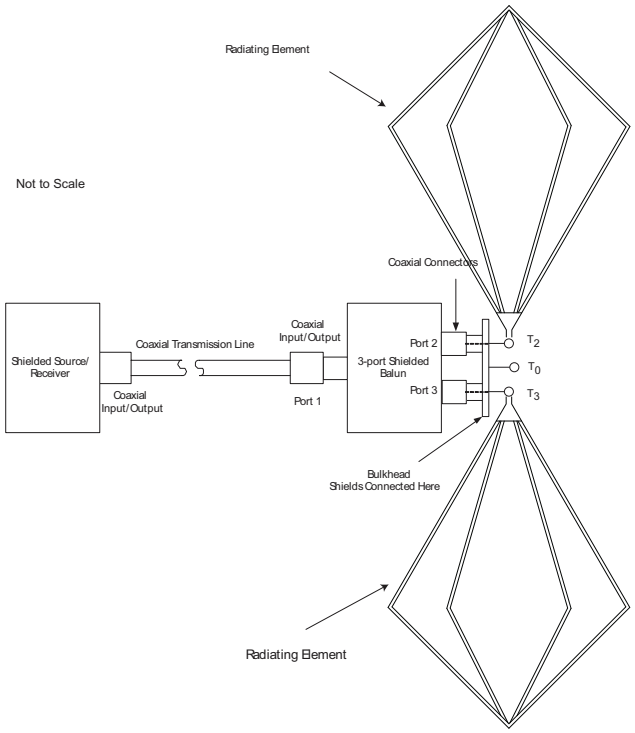

Fig. 2. Biconical antenna driven by 3-port, shielded, "connectorized" balun: The location of the three terminals for a sound physical port representation are indicated by T_0, T_2, and T_3 [11]. Port 2 comprises terminals T_2 and T_0 while port 3 comprises terminals T_3 and T_0.

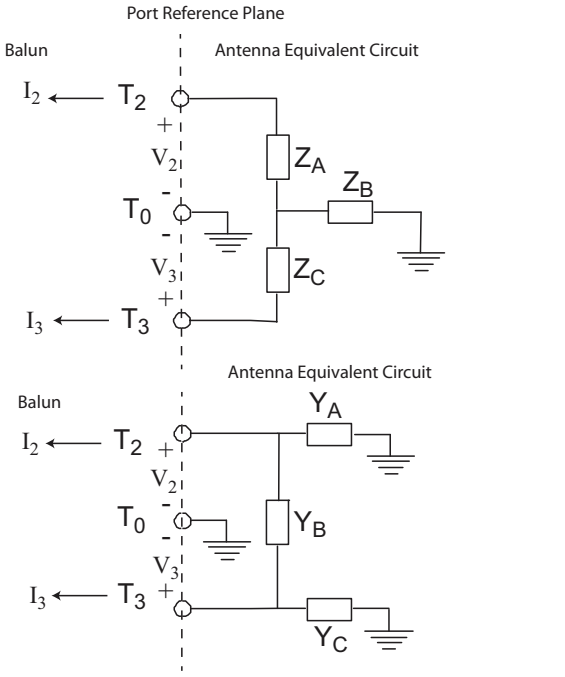

Fig. 3. Equivalent T and Π networks for the terminals shown in Fig. 2. The terminals and ports correspond to those in Fig. 2. The positive current direction for each port is into the port of the balun and thus out of the equivalent network of the antenna.

impedance, i.e. $Y_A = Y_C = 0$, representation of the above-described antenna is very much inadequate. The 2-terminal load representation itself enforces current balance and thus, cannot represent imperfect operation of the balun. This is true even for horizontal polarization where the load is symmetric, i.e. $Y_A = Y_C \neq 0$. In this case, a finite common-mode antenna input impedance, $Z_{CM} = (Y_A + Y_C)^{-1}$, will allow an asymmetric balun to drive unbalanced currents. Of course, the isolated, 2-terminal impedance will not.

A rigorous definition of balun is prerequisite to a formal discussion of balance and symmetry. We define a balancing network or balun as a 3-port network with port 1 being the input that enforces balance of one of a pair of power-conjugate variables [10], [12] (e.g. voltage, current, power-normalized wave amplitude) at the output ports, ports 2 and 3. The other power-conjugate variable at each output port is then determined by the load. For example, voltage can be balanced at ports 2 and 3 leaving the currents to be determined by the 3-terminal load or currents can be balanced at ports 2 and 3 leaving the voltage to be determined by the load. Each of these fundamental balun types can be most naturally represented by its native 3-port matrix representation: For example, the current balun would be represented by an admittance matrix with the following form:

$$\begin{bmatrix} I_1 \\ I_2 \\ I_3 \end{bmatrix} = [Y] \begin{bmatrix} V_1 \\ V_2 \\ V_3 \end{bmatrix} = \begin{bmatrix} A & B & -B \\ B & C & -C \\ -B & -C & C \end{bmatrix} \cdot \begin{bmatrix} V_1 \\ V_2 \\ V_3 \end{bmatrix}, \tag{1}$$

where A, B, and C are complex, frequency-dependent admittances. Note that for a lossless 3-port network, these admittance parameters would be purely imaginary and thus, the matrix could be written with a scalar factor of j multiplying a purely real matrix. Also note that the corresponding impedance matrix for the lossless 3-port network would also be purely imaginary. One can see from Eqn. 1 that $I_3 = -I_2$ for any load configuration. If the balun of the vertically-polarized antenna referred to earlier has the admittance matrix representation in Eqn. 1, no amount of coupling to the ground including the tip of the lower element making galvanic contact to the ground can cause the balun output currents to be unbalanced. An ideal voltage balun would naturally be represented by an impedance matrix with the same form as Eqn. 1. However, one might notice that the matrix in Eqn. 1 is singular and thus the impedance matrix representation of a current balun does not exist. The 180° power divider (which balances outgoing power-normalized wave amplitudes at ports 2 and 3) would be represented by a scattering matrix with the same form. All three fundamental balun types can be represented by a scattering matrix as will be shown. These considerations were presented in basic form in ref. [1]. In this extended paper, additional simulations and the effects of symmetry and balance

on radiation pattern are presented. Specifically, it is shown that in some cases trading current balance for symmetry with a vertically-polarized antenna results in radiation pattern distortion. Because it is not always possible to obtain acceptable symmetry and simultaneously voltage or current balance, an analysis is presented which determines the physical quantity is balanced by a general symmetric balun; that is, a symmetric balun which is neither a voltage nor a current balun. Finally, a discussion of the sensitivity of symmetry to imbalance in current baluns is included along with an illustrative example.

II. Common-mode Current on the Exterior of the Feed Transmission Line

Clearly, minimizing CM current on the exterior of the feed transmission line is of some value. It is worthwhile to recognize that it is very difficult to completely "choke off" the feed transmission line exterior with ferrite clamps if the arrangement of antenna, balun, and feed transmission line is conducive to CM current. On one hand, antenna-to-antenna transmission between balun driven dipolar antennas operating over a ground plane constitutes one large electromagnetic system which must be analyzed simultaneously. However, it is useful and not unsound to delineate two sources of CM current on the exterior of the feed transmission line. One is the induction or excitation of CM current by the external electromagnetic field from the antennas, including both near-field and far-field coupling. The other is imbalance of currents at the bases of the two halves (the center) of the antenna under test. While the illumination of the feed transmission line by the antennas cannot be avoided, balance of currents at the bases of the dipolar elements can be enforced. We assume that the antenna base currents, the currents at the vertices of the two halves of the biconical antenna, are equal to the currents on the center conductors of their respective balun ports, ports 2 and 3. This involves a tacit assumption that the lengths of the electrical connections between the balun output ports and the antenna element bases are very short, but this should be the case for a metrology antenna which is intended to give "calculable" performance or rather performance which can be predicted by a relatively simple model. Following standard practice for multi-port network representations, I_2 and I_3 are taken as positive going into their respective port. Balancing the currents at the bases of the dipole elements, I_2 and I_3, thus minimizes (not eliminates) the CM current $I_{CM} = I_2 + I_3$ on the exterior of the balun as shown in Fig. 4. Only true current balancing action will eliminate this component of the CM current if the effective 3-terminal load is asymmetric. Of course this is only true if the continuity equation reduces to Kirchoff's current law for the control volume. Referring to Fig. 4, that is:

$$-\int_S \vec{J}\cdot d\vec{S} \;=\; I_2 + I_3 - I_{CM} = \frac{\partial}{\partial t}\int_V \rho dV = 0. \quad (2)$$

Thus, we state unequivocally that a current balun is preferable if such a device is in fact available because it minimizes the CM current due to imbalance at the bases of the dipole elements. The CM current caused by illumination of the feed transmission line is then reduced by proper arrangement of the feed transmission line, in particular the horizontal portion of the line extending back from the balun.

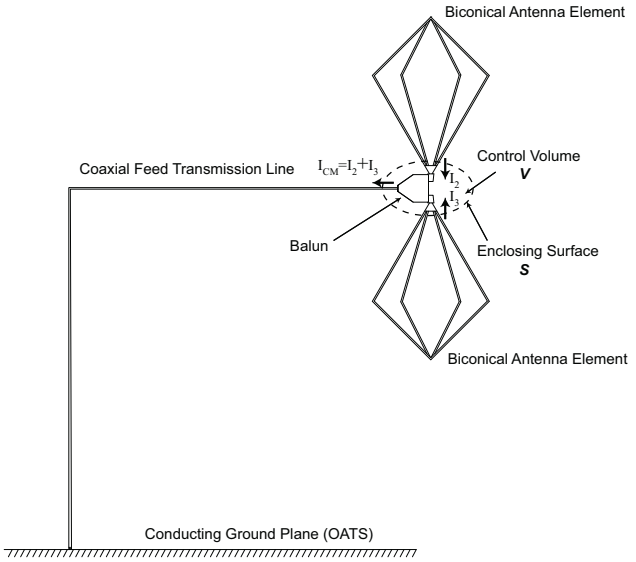

Fig. 4. Biconical antenna in vertical polarization above conducting ground plane. The CM current on the feed transmission line is $I_{CM} = I_2 + I_3$.

III. Antenna Symmetry

If the dipole elements in Fig. 1 and Fig. 4 are themselves identical and thus symmetric and the feed transmission line properly laid out, any asymmetry that exists in the system must be due to the three-port balun of the AUT. To see this consider Fig. 5 which depicts a thought experiment in which the AUT radiating elements and feed transmission line are somehow fixed into place and AUT balun alone is rotated or inverted. The original inversion test should give identical results to this one if the AUT radiating elements are identical and the feed transmission line is not disturbed. To satisfy the balance tests in ref. [2] and [3], assuming the dipolar elements are identical, it is necessary then that an interchange of ports 2 and 3 of the balun causes no (or acceptable) change in the insertion loss. That is, inverting the AUT can be thought of as interchanging ports 2 and 3 of the AUT balun. If the 3-port representation (e.g. S,Z,Y) of a linear time-invariant network has the following symmetry, interchange of ports 2 and 3 has no effect:

$$[S] \;=\; \begin{bmatrix} C & A & A \\ A & B & D \\ A & D & B \end{bmatrix}. \quad (3)$$

This can be seen by interchanging rows 2 and 3 and then interchanging columns 2 and 3.

A. Pathological Case: Symmetry but no balance

If phase sensitive detection is not employed and the balance tests consists of simply comparing the magnitudes of the two

sets of insertion loss data measured as in Fig. 1, the pathological limiting case of an unmatched coaxial T employed in lieu of a balun satisfies the scalar symmetry test as can be seen from its scattering representation in Eqn. 4. This can be seen from the scattering representation of an ideal coaxial T:

$$[S] = \begin{bmatrix} 1/3 & 2/3 & 2/3 \\ 2/3 & 1/3 & 2/3 \\ 2/3 & 2/3 & 1/3 \end{bmatrix}. \quad (4)$$

In fact, if such an unmatched T replaced the balun in the AUT in Fig. 1, the AUT would pass the symmetry test albeit with a poor (but still finite) antenna factor. The AUT would have only common-mode operation but due to its geometry would receive some vertical polarization from the transmitting antenna. Inverting the AUT would have no effect at all.

B. Antisymmetry

On the other hand, if any of the previously-mentioned 3-port representations of a balun has the following symmetry, interchange of ports 2 and 3 has the effect of changing the source phase by 180°:

$$[S] = \begin{bmatrix} C & A & -A \\ A & B & D \\ -A & D & B \end{bmatrix}. \quad (5)$$

This form would then satisfy the requirement that the magnitude of the insertion loss remain constant with inversion while the insertion phase change 180° with inversion. In summary, the symmetry test is not really a test of balancing action but only of the symmetry of the balancing network. Of course, a balun must be symmetric in order to be able to provide voltage or current balancing, but symmetry alone does not imply balance of any voltage or current when the balun is connected to an asymmetric load. Symmetry is necessary but not sufficient to enforce current balance at the dipole feed. Since the trivial case of symmetry with no balance is not important, we use the term symmetry from here on to imply antisymmetry as defined by Eqn. 5.

In general the matrix in Eqn. 5 is not singular. Clearly, if $B = -D$, the matrix takes on the form of Eqn. 1 and is singular. However, even if $B \neq -D$, the matrix can still be singular if a pathological relation exists between A, B, C, and D. The determinant is $\Delta S = C\left(B^2 - D^2\right) - 2A\left(AD + AB\right)$. The inverse of this matrix is given in Eqn. 6:

$$[S]^{-1} = \frac{1}{\Delta S}\begin{bmatrix} C' & A' & -A' \\ A' & B' & D' \\ -A' & D' & B' \end{bmatrix}, \quad (6)$$

where

$$A' = -\left(AB + AD\right), \quad (7)$$
$$B' = \left(BC - A^2\right), \quad (8)$$
$$C' = \left(B^2 - D^2\right), \text{ and} \quad (9)$$
$$D' = -\left(CD + A^2\right). \quad (10)$$

Note that if the original matrix is not singular, the inverse has exactly the same form. This property will be shown to be quite important in the following sections, but one example can be immediately seen: If one designs a balun with a nonsingular admittance matrix possessing the symmetry of Eqn. 5, it will behave symmetrically under short-circuit conditions with the short-circuit output currents balancing. Still, is not a true current balun as it will not enforce current balance under all load conditions. However, Eqn. 6 predicts that it will also behave symmetrically under open-circuit conditions with the open-circuit voltages balancing as well. Nevertheless, it is not a voltage balun either. In fact, it will be seen that avoidance of true current or voltage balancing action results in more symmetric performance under generalized load conditions.

IV. Baluns derived from 180° 4-Port Hybrids

In this section we will show that any balun derived from a 4-port 180° hybrid satisfies Eqn. 5. The 4-port 180° hybrid network has two pairs of conjugate or isolated ports In ref. [10] it was shown that if one begins with such a 4-port 180° hybrid, takes one of the delta ports as the input, and terminates the corresponding sum port in any passive load, a symmetric (actually anti-symmetric) 3-port will be obtained:

$$[S] = \frac{1}{\sqrt{2}}\begin{bmatrix} 0 & 1 & -1 \\ 1 & \frac{\Gamma}{\sqrt{2}} & \frac{\Gamma}{\sqrt{2}} \\ -1 & \frac{\Gamma}{\sqrt{2}} & \frac{\Gamma}{\sqrt{2}} \end{bmatrix}. \quad (11)$$

Thus, a representation of a very general 3-port balun is obtained. Clearly for any complex value of Γ this network will be antisymmetric and pass the mandated tests in ref. [2], [3] as it has the same form as Eqn. 5. However, Eqn. 11 is not completely general since it is not necessary for the balun to be matched at the input port. The most general balun topology which satisifies Eqn. 5 can be derived from the lumped hybrid transformer [13]–[15] is shown in Fig. 6. The scattering matrix

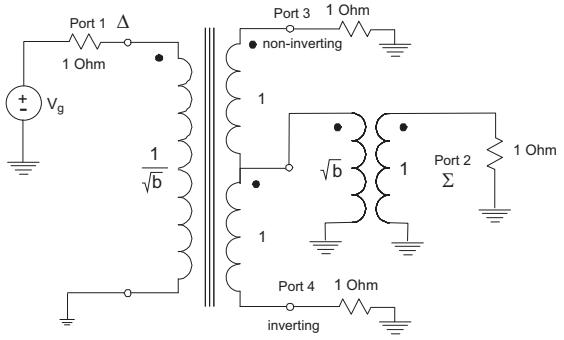

Fig. 6. Lumped hybrid transformer as portrayed in Fig. 4.12 (b) of ref. [15] or Fig 1 of ref. [14].

this ideal lumped hybrid transformer or hybrid coil is [15]:

$$[S] = \begin{bmatrix} \alpha & 0 & \beta & -\beta \\ 0 & \alpha & \beta & \beta \\ \beta & \beta & -\alpha & 0 \\ -\beta & \beta & 0 & -\alpha \end{bmatrix} \quad (12)$$

where $\alpha = \frac{1-2b}{1+2b}$, $\beta = \frac{2\sqrt{b}}{1+2b}$, and b is the square of the turns ratio of one of the two identical secondary windings

to the primary winding. This real scattering matrix could be generalized to the complex case by adding equal transmission line lengths to two (either of the two conjugate pairs) or all four of the ports. Finally, two arbitrary but identical all-pass networks could be added to either or both pairs of conjugate ports. This addition would also make the scattering matrix complex. Now if port 2 (the sum port) is connected to a load with reflection coefficient Γ a 3-port balun is obtained with the following scattering representation:

$$[S] = \begin{bmatrix} \alpha & \beta & -\beta \\ \beta & \frac{\beta^2\Gamma}{1-\alpha\Gamma} - \alpha & \frac{\beta^2\Gamma}{1-\alpha\Gamma} \\ -\beta & \frac{\beta^2\Gamma}{1-\alpha\Gamma} & \frac{\beta^2\Gamma}{1-\alpha\Gamma} - \alpha \end{bmatrix}. \quad (13)$$

If $b = \frac{1}{2}$ then $\alpha = 0$ and the hybrid is matched at all ports and the 3-port balun scattering matrix becomes Eqn. 11, but in any case it has the same form as Eqn. 5 regardless of whether the input is matched.

V. Exploitation of Phase-Sensitive Detection

In general, the phase (for example of scattering parameters) is a more sensitive function than the amplitude and more readily reveals deviation from ideal behavior. However, if phase sensitive-detection, e.g. a vector network analyzer, is available, a much more sensitive quantity can be defined by noting that:

$$S_{21}^{up} + S_{21}^{dn} = 0, \text{ ideally} \quad (14)$$

and

$$S_{21}^{up} - S_{21}^{dn} = 2S_{21}^{up} = -2S_{21}^{dn}, \text{ ideally,} \quad (15)$$

where the superscript up denotes the AUT in one (up) vertical orientation and the superscript dn denotes the AUT in the other (down) orientation. In ref. [2] the magnitudes of these two quantities are referred to as A_{0° and A_{180°, respectively. In ref. [3] the magnitudes of these two quantities are referred to as U_1 and U_2, respectively. It is important to note that here S_{21}^{up} and S_{21}^{dn} are being added and subtracted, not ratioed or divided and thus are not expressed in dB. A parameter similar to common-mode rejection ration (CMRR) could then be expressed as:

$$\text{CMRR (dB)} = 20\log_{10}\left(\frac{S_{21}^{up} - S_{21}^{dn}}{S_{21}^{up} + S_{21}^{dn}}\right). \quad (16)$$

This parameter is ideally infinite as it would be for Eqn. 5 and in the worst case, Eqn. 4, zero ($-\infty$ dB) like conventional common-mode rejection. The primary problem with the direct application of Eqn. 16 to the symmetry tests in ref. [2] and ref. [3] is that if vertical scanning is employed to mitigate transmission nulls due to reflection from the ground plane, the maximum could be achieved at different heights for the two vertical orientations. Of course this is a problem even when phase sensitive detection is not used. If an antenna is perfectly symmetric, the z location of the transmission maximum in one vertical orientation will be the same as the for the other orientation. However, this is not generally true if some asymmetry exists. In fact, a pathological case of asymmetry could exist in which the ratio of transmission scattering parameters was unity but obtained at different heights for the two orientations. That is, it is not proper to compare the transfer scattering parameters when the maxima are not at the same height. In Fig. 7 the magnitude of the ratio of the transfer scattering parameters measured in a balun inversion test for two 1.4-meter biconical antennas separated by 3 meters and at a fixed height of 0.8 meters above ground are plotted. In Fig. 8 the quantity given in

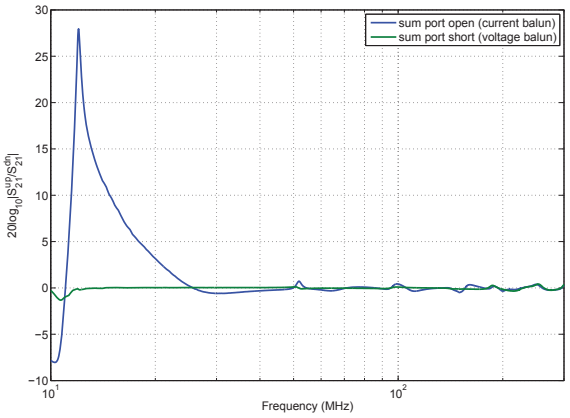

Fig. 7. Ratio of transmission scattering parameters $\left|\frac{S_{21}^{up}}{S_{21}^{dn}}\right|$ in balun inversion test as computed with HFSS.

Eqn. 16 for the same transfer scattering parameters is plotted. What is not obvious from Fig. 7 is that although there are 8

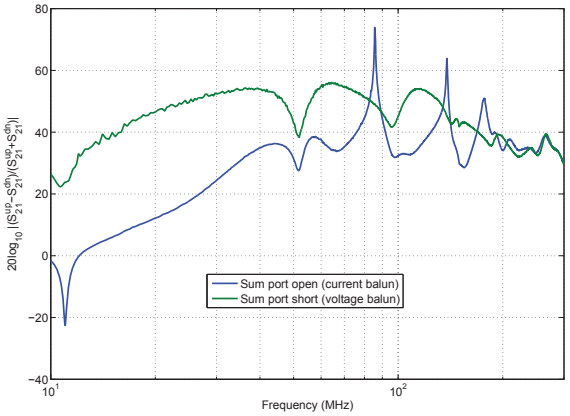

Fig. 8. Eqn 16 from balun inversion test in Fig. 7 as computed with HFSS.

zero crossings (unity magnitude or 0 dB) for the $\left|\frac{S_{21}^{up}}{S_{21}^{dn}}\right|$ data obtained with a voltage balun and 17 for the data obtained with a current balun, the CMRR is finite at all frequencies and there are only two frequencies at which the CMRR is greater than 60 dB as can be seen in Fig. 8. This is because when the ratio of the magnitudes is unity the phase is not exactly 180°.

VI. Manifestation of Imbalance in Pattern

Clearly, the entire hemispherical pattern of an antenna operating over ground is required to fully understand its operation. Unfortunately, such comprehensive information is not easily obtainable for most test laboratories and thus practical compromises such as the symmetry tests prescribed in ref. [2] and [3] are made. In this section, with the aid of numerical simulation, we consider the effect of the balun type on the pattern of a vertically-polarized biconical antenna on an OATS. As noted earlier, a symmetric balun does not necessarily enforce current balance when the antenna is asymmetrically influenced and hence 2-port antenna model is asymmetric. Consider a vertically-polarized 1.4-m biconical antenna situated 1 m above a conducting ground plane with a coaxial feed transmission line extending horizontally 1.5 and then vertically to ground as described in Section V. Using a numerical simulation it is possible to compute the electromagnetic field of the antenna for three cases: (1) ideal current balun, (2) ideal voltage balun, and (3) a ideal 180° power divider. For the geometry of the antenna and feed line, it is the E-plane pattern that is of most interest. The E-plane is shown explicitly in Fig. 9 The E-plane (y-z plane) is the plane

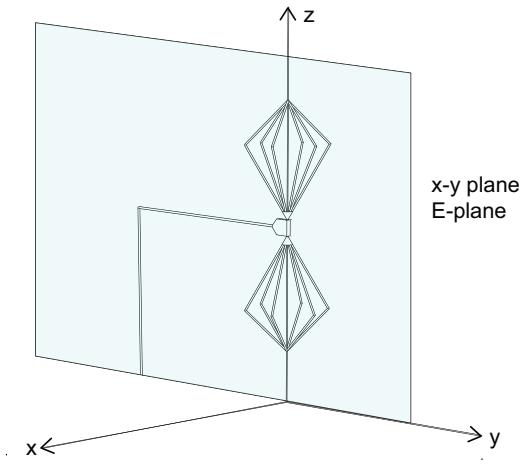

Fig. 9. E-plane of vertically-polarized biconical antenna over ground. Note that the feed transmission line lies completely within the E-plane. The ground plane is the x-y plane.

containing the axis of the biconical antenna and the horizontal portion of the feed transmission line. The H-plane (parallel to x-y plane and containing the feed point) pattern absent the feed line is omnidirectional and therefore is less strongly affected by imbalance. However, it is still changed slightly by lack of current balance at the balun.

A Thévenin or Norton 2-port equivalent is needed for the simulation. Such a representation has been given in ref. [16]. In Fig. 10, the 2-port Thévenin representation is given. As can be seen, the Thévenin equivalent networks of all three are symmetric. For a current balun, $Z_B = \infty$ and $Z_A = Z_C = Z_0$. For a voltage balun, $Z_B = -\frac{Z_0}{2}$ and $Z_A = Z_C = Z_0$. For a hybrid with the sum port terminated or 180° power divider, $Z_B = 0$ and $Z_A = Z_C = Z_0$. All three baluns can then

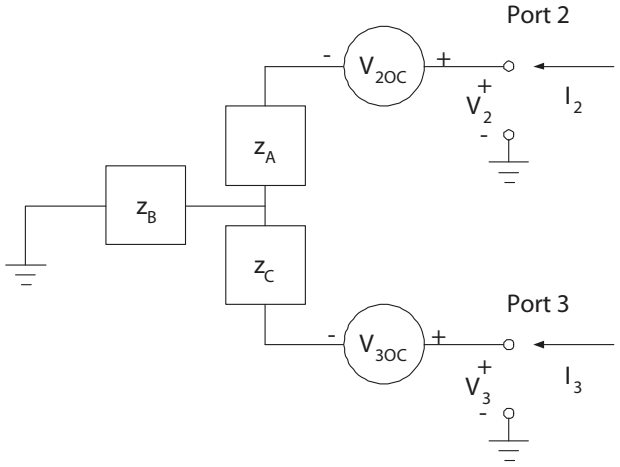

Fig. 10. Thévenin equivalent network for a reciprocal 3-port balun.

be easily represented in a numerical simulation, in this case HFSS, using lumped voltage sources and loads.

In Fig. 11 the E-plane patterns obtained with ideal voltage and current baluns is shown. As can be seen at $\theta = 0$, where a null would be if the pattern were dipolar, a large difference exists between the two patterns. However, on the bore sight, the difference is only .6 dB.

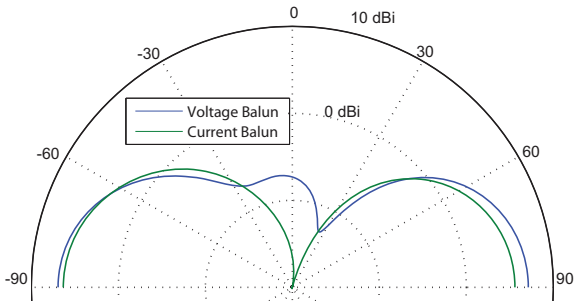

Fig. 11. E-plane pattern of vertically-polarized biconical antenna driven by voltage and current baluns.

A series of E-plane patterns obtained with a 180° hybrid having the sum port terminated is presented in Fig. 12. In Fig. 12, the normalizing impedance of the hybrid is varied from 25 to 800 Ohms. Because the 2-port Thévenin equivalent circuit for the hybrid consists simply of a push-pull pair of two 1-port Thévenin sources [16], as the normalizing impedance is increased the system behaves more like two ideal current sources and the pattern approaches that obtained with a current balun. Note however, that the overall action is not the same as the input match is very much degraded. It is interesting to note that even an ideal current balun cannot force the E-plane pattern to be perfectly dipolar. This is due to field coupling to the vertical portion of the feed line. To better understand the affect on the total radiation pattern by the balun topology, 3-dimensional radiation patterns for the vertical biconical antenna at 60 MHz driven by a current and a voltage balun

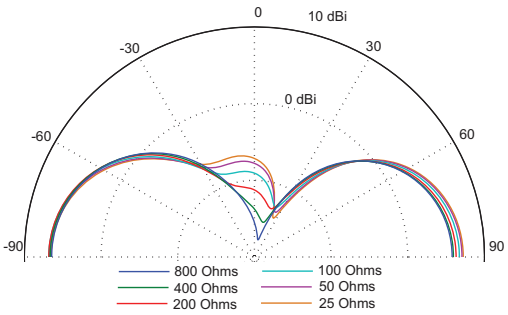

Fig. 12. E-plane pattern of vertically-polarized biconical antenna driven by 180° hybrid with the sum port terminated.

are shown in Fig. 13 and Fig. 14, respectively. In Fig. 13 and Fig. 14 the radial scale is linear in order to facilitate viewing the detail in the patterns. In Fig. 15, the E-plane

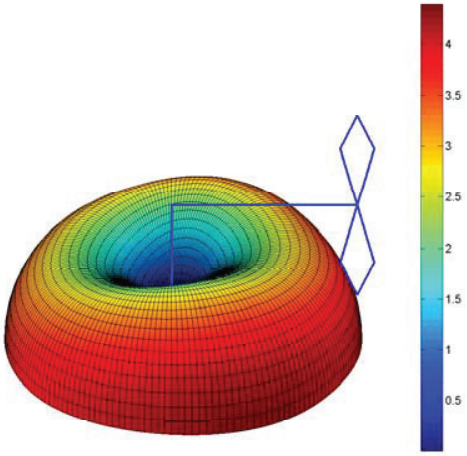

Fig. 13. 3-dimensional radiation pattern depicting the total gain of the vertically-polarized biconical antenna driven by a current balun at 60 MHz.

pattern for the vertical biconical antenna at 55 MHz is shown. As can be seen, the voltage and current baluns give similar patterns and the patterns are nearly dipolar. This is because the CM impedance of the entire structure is very large near 55 MHz. The CM impedance is shown in Fig. 16. It is important to remember that all the baluns in Figs. 11, 12, and 15 are perfectly symmetric. Only the current balun gives a quasi-dipolar pattern at 60 MHz. The pattern at 55 MHz is primarily due to the self-balancing effect [17].

VII. Generalization of Balun Symmetry

A remaining question pertains to what quantity, if any, is balanced by a generalized symmetric 3-port balun. For example, a 3-port balun could exhibit a symmetric, 3-port

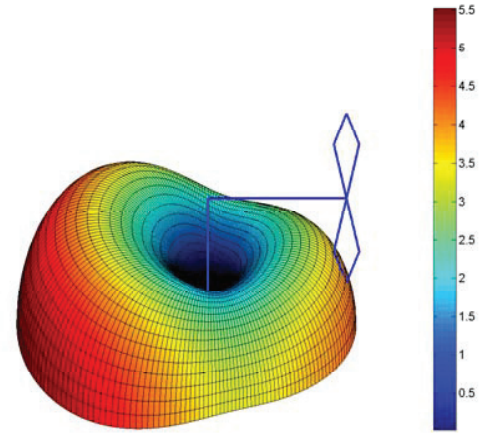

Fig. 14. 3-dimensional radiation pattern depicting the total gain of the vertically-polarized biconical antenna driven by a voltage balun at 60 MHz.

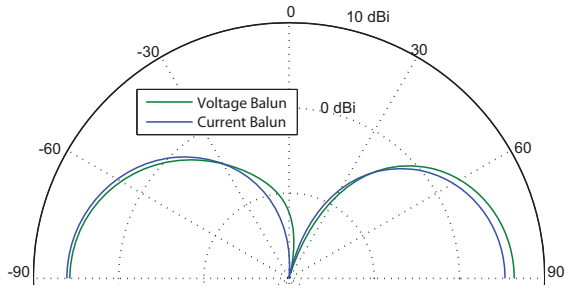

Fig. 15. E-plane pattern of vertically-polarized biconical antenna driven by voltage and current baluns at 55 MHz.

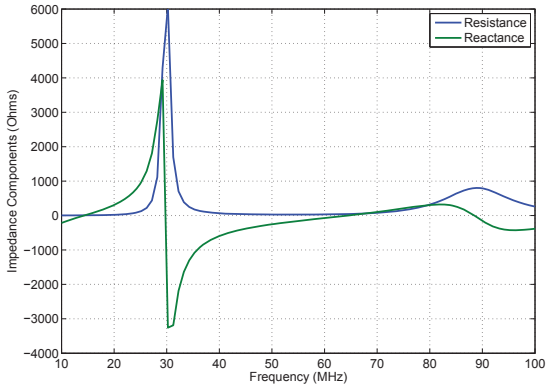

Fig. 16. Common-mode impedance of biconical antenna driven against exterior of feed transmission line.

admittance matrix of the form in Eqn. 5 which does not satisfy

the stricter requirements for a current balun given in Eqn. 1:

$$\begin{bmatrix} I_1 \\ I_2 \\ I_3 \end{bmatrix} = [Y] \begin{bmatrix} V_1 \\ V_2 \\ V_3 \end{bmatrix} = \begin{bmatrix} C & A & -A \\ A & B & -D \\ -A & -D & B \end{bmatrix} . \begin{bmatrix} V_1 \\ V_2 \\ V_3 \end{bmatrix} \tag{17}$$

where $B \neq D$. The symmetry in the matrix here is the same as that in Eqn. 5, but it is written this way to facilitate exposition. One can immediately show that the inverse of a matrix with the symmetry properties of Eqn. 5 also exhibits the same symmetry properties. Thus, if the impedance matrix representation satisfies Eqn. 5 then the admittance matrix representation does as well. Moreover, the scattering matrix will also exhibit the same symmetry.

To understand what physical quantity is balanced, we define a new vector of port variables:

$$\begin{bmatrix} X_1^+ \\ X_2^+ \\ X_3^+ \end{bmatrix} = \begin{bmatrix} I_1 - (B-D)\, V_1 \\ I_2 - (B-D)\, V_2 \\ I_3 - (B-D)\, V_3 \end{bmatrix} \tag{18}$$

and substitute them into Eqn. 17:

$$\begin{bmatrix} X_1^+ \\ X_2^+ \\ X_3^+ \end{bmatrix} = \begin{bmatrix} C-B+D & B & -B \\ B & D & -D \\ -B & -D & D \end{bmatrix} \begin{bmatrix} V_1 \\ V_2 \\ V_3 \end{bmatrix} . \tag{19}$$

Eqn. 19 has the same form as Eqn. 1. Thus, it is X_2^+ and X_3^+ that are balanced by such a network. That is, $X_3^+ = -X_2^+$ regardless of V_1, V_2, and V_3. The quantity X_i^+ resembles a scattering variable. However, it should be kept in mind that B and D can be complex. In summary, such a symmetric 3-port network does in fact balance a physical quantity at the two output ports. In the case above this quantity differs the port current, but still has units of Amperes. If $B - D = \frac{1}{Z_0}$, it would be the outgoing current wave complex amplitude, but again, the result is more general than this. The analysis can be taken further to show that

$$\left[X^+\right] = \underbrace{\left[[Y] - (B-D)\,[E]\right]}_{\text{balanced: Eqn. 1}} \underbrace{\left[[Y] + (B-D)\,[E]\right]}_{\text{symmetric: Eqn. 5}}^{-1} \left[X^-\right] \tag{20}$$

where $[E]$ is the identity matrix and $[X^-] = [I] + (B-D)\,[V]$. It can easily be shown that the matrix product in Eqn. 20 which is the product of a matrix with the form of Eqn. 1 and Eqn. 5 exhibits the same symmetry as Eqn. 1; that is, it has the form of a balun enforcing balance for X^+. Also note that the matrix is singular. Finally, note that X^- will be balanced only if the load is symmetric.

In view of the forgoing discussion and Eqns. 18 and 19, Eqn. 11 can be rewritten as:

$$\begin{bmatrix} b_1 - \Gamma a_1 \\ b_2 - \Gamma a_2 \\ b_3 - \Gamma a_3 \end{bmatrix} = \frac{1}{\sqrt{2}} \begin{bmatrix} -\sqrt{2}\Gamma & 1 & -1 \\ 1 & -\frac{\Gamma}{\sqrt{2}} & \frac{\Gamma}{\sqrt{2}} \\ -1 & \frac{\Gamma}{\sqrt{2}} & -\frac{\Gamma}{\sqrt{2}} \end{bmatrix} \begin{bmatrix} a_1 \\ a_2 \\ a_3 \end{bmatrix} . \tag{21}$$

One might step back and examine Eqn. 21. If port 1 is driven by a typical RF source, a_1 is set. This is equivalent to driving the balun with a Thévenin source with impedance Z_0. One would typically think that at the output a_2 and a_3, the incoming waves at ports 2 and 3, are determined by the 2-port load and the outgoing waves, b_2 and b_3. While this is true, as can be seen the quantities $b_2 - \Gamma a_2$ and $b_3 - \Gamma a_3$ are what is being forced equal in magnitude and opposite in phase. The quantity $b_i - \Gamma a_i$ is the port voltage when $\Gamma = -1$, the port current when $\Gamma = 1$, and the outgoing power-normalized wave amplitude when $\Gamma = 0$. However, Eqn. 21 has the form of Eqn. 5 for any value of Γ indicating balance for the port quantities $(b_2 - \Gamma a_2)$ and $(b_3 - \Gamma a_3)$. Thus, an ideal 180° hybrid network with a generalized complex termination at the sum port is such a generalized symmetric balun. Finally, it is useful to notice that if in Eqn. 21, $B - D \neq 0$ and the 3-port balun balances some linear combination of voltage and current then under short-circuit conditions the currents are balanced and under open-circuit conditions the voltages are balanced.

VIII. Sensitivity

In this section we analyze a current balun with a very slight short-circuit current imbalance, but otherwise nearly ideal behavior, in order to show the sensitivity of the open-circuit voltages to minor imperfections. This situation occurs in the presence of inter-winding capacitance as is shown in ref. [18]. Consider Eqn. 4 from ref. [19] which is the admittance matrix for a conventional or Faraday 3-port isolation transformer or current transformer:

$$[Y] \;=\; \frac{1}{j\omega\,(L^2 - M^2)} \begin{bmatrix} L & -M & M \\ -M & L & -L \\ M & -L & L \end{bmatrix} . \tag{22}$$

Again, note that this matrix is complex, but pure imaginary as the transformer is taken as lossless. Now suppose a small inter-winding capacitance exists between the primary and secondary. A sound lumped-element representation would consist of two equal capacitances connecting the primary and secondary windings as shown in Fig. 17. The dot arrangement

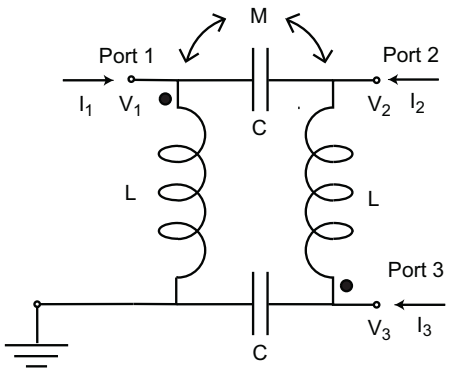

Fig. 17. Faraday transformer with inter-winding capacitance. The dot arrangement or relative sense of the windings corresponds to the numerical example in this section.

or relative sense of the windings in Fig. 17 corresponds to the numerical example in this section. The relative sense of the windings has some effect on the inter-winding capacitance.

With the inter-winding capacitance, the admittance matrix representation becomes:

$$[Y] = \begin{bmatrix} \frac{1}{j\omega L\delta} + j\omega C & \frac{-k_m}{j\omega L\delta} - j\omega C & \frac{k_m}{j\omega L\delta} \\ \frac{-k_m}{j\omega L\delta} - j\omega C & \frac{1}{j\omega L\delta} + j\omega C & \frac{-1}{j\omega L\delta} \\ \frac{k_m}{j\omega L\delta} & \frac{-1}{j\omega L\delta} & \frac{1}{j\omega L\delta} + j\omega C \end{bmatrix} \tag{23}$$

where $k_m = \frac{M}{L}$ is the magnetic coupling coefficient. and $\delta = \left(1 - k_m^2\right)$. Note that k_m and δ are dimensionless. Suppose that the magnitude of the contribution to Y_{12} from the inter-winding capacitance is a small fraction Δ of the original entry $\frac{-k_m}{j\omega L\delta}$:

$$\omega C \quad = \quad \Delta \frac{k_m}{\omega L\delta}. \tag{24}$$

Note that Δ is dimensionless. Also, note that for Y_{12} the term due to C subtracts from the original entry in Eqn. 22 for the dot arrangement or relative winding sense shown in Fig. 19, while for Y_{11} it subtracts from the original entry in Eqn. 22, regardless of the relative winding sense. This term is absent for Y_{13} and thus degrades short circuit current balance. However, since Δ is small, this imbalance is slight. Given a specific frequency, the value of C that would result in this is:

$$C \quad = \quad \Delta \left(\frac{1}{\omega^2 L}\right)\left(\frac{k_m}{\delta}\right). \tag{25}$$

Given a value for L, k_m, and C, this condition would occur at a radian frequency of:

$$\omega \quad = \quad \sqrt{\Delta \left(\frac{1}{LC}\right)\left(\frac{k_m}{\delta}\right)}. \tag{26}$$

This slightly asymmetric current balun could have the following admittance matrix representation where a slight 1% imbalance exists in the short-circuit current:

$$[Y] = \frac{1}{j\omega L\delta}\begin{bmatrix} 0.9901 & -0.9801 & 0.9900 \\ -0.9801 & 0.9901 & -1.0000 \\ 0.9900 & -1.0000 & 0.9901 \end{bmatrix}. \tag{27}$$

The condition number of this matrix, $\|Y\|_2 \|\mathrm{inv}(Y)\|_2$, is approximately 259.8 [20]. The inverse of this matrix is the impedance matrix and gives the open-circuit voltage behavior:

$$[Z] = \mathrm{inv}\,[Y] = j\omega L\begin{bmatrix} 1.0000 & 0.9950 & 0.0050 \\ 0.9950 & -0.0101 & -1.0051 \\ 0.0050 & -1.0051 & -1.0000 \end{bmatrix}. \tag{28}$$

Obviously, the open-circuit output voltages are not balanced at all. A slight asymmetry in the admittance matrix causes a large asymmetry in the impedance matrix. Now consider a similar balun which is symmetric but has only the non-ideal current balun behavior in the diagonal entries for the output ports. That is, the short-circuit currents are balanced, but current balun behavior is not perfectly maintained for all 2-port loads due to imperfect coupling between the output ports. Such behavior can be obtained from the current transformer when an electrostatic shield [21] is placed between the primary and secondary as described in ref. [18]. This results in a topology as shown in Fig. 18.

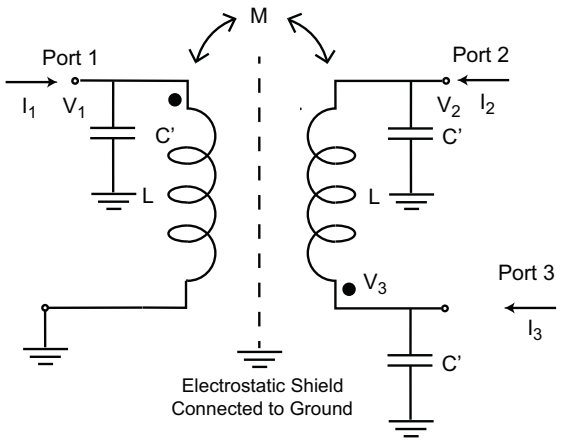

Fig. 18. Faraday transformer with a grounded electrostatic shield between the primary and secondary.

$$[Y] = \begin{bmatrix} \frac{1}{j\omega L\delta} + j\omega C' & \frac{-k_m}{j\omega L\delta} & \frac{k_m}{j\omega L\delta} \\ \frac{-k_m}{j\omega L\delta} & \frac{1}{j\omega L\delta} + j\omega C' & \frac{-1}{j\omega L\delta} \\ \frac{k_m}{j\omega L\delta} & \frac{-1}{j\omega L\delta} & \frac{1}{j\omega L\delta} + j\omega C' \end{bmatrix} \tag{29}$$

$$[Y] = \frac{1}{j\omega L\delta}\begin{bmatrix} 0.9802 & -0.9900 & 0.9900 \\ -0.9900 & 0.9802 & -1.0000 \\ 0.9900 & -1.0000 & 0.9802 \end{bmatrix}. \tag{30}$$

In fact this matrix, Eqn. 30, is less well conditioned than Eqn. 30; the condition number is 458.2. However, now $Y_{13} = -Y_{12}$ and thus, the short-circuit currents are balanced. The deviation from true current balun behavior is instead due to $Y_{22} \neq -Y_{32}$.

$$[Z] = \mathrm{inv}\,[Y] = j\omega L\begin{bmatrix} -2.0515 & -1.0257 & 1.0257 \\ -1.0257 & -1.0103 & 0.0052 \\ 1.0257 & 0.0052 & -1.0103 \end{bmatrix}. \tag{31}$$

Now, the open-circuit output voltages are balanced and in fact the S, Y, and Z matrices satisfy Eqn. 5. But, it should be noted that the deviation from current balun behavior in Eqn. 30, specifically the relationship between the Y_{22} and Y_{32} entries, is extremely slight. Also, it should be noted that Eqn. 31 does not imply voltage balancing under all load conditions because $Z_{32} \neq -Z_{22}$. In fact $|Z_{32}|$ is very small compared to $|Z_{22}|$. To summarize: in the ideal case without the shield and without the inter-winding capacitance, the current balancing is perfect. However, with the inter-winding capacitance, the current balancing is imperfect and the balun is slightly asymmetric in terms of short-circuit currents, but highly asymmetric in terms of open-circuit voltages. With the inter-winding capacitance and the shield, symmetry is restored, but the current balance for asymmetric 2-port loads is slightly imperfect. However, this is clearly the best approach as it involves tolerating

only a very slight deviation from true current balun behavior in exchange for symmetry. Thus, in conclusion, instead of attempting to make a perfect voltage or current balun it is better to seek near-perfect symmetry for the two extremes, short-circuit current and open-circuit voltage, and then accept some slight deviation from current or voltage balancing in the relationship between the diagonal and off-diagonal entries of the matrix representation of the balun. This amounts to a slight adjustment of the coupling between the output ports. Such a balun will satisfy the symmetry requirements in refs. [2] and [3] and result in better performance with a wide range of symmetric and asymmetric 2-port loads.

A. Simple Numerical Example

A simple Faraday transformer as shown in Fig. 19 was modeled using the commercial finite element simulation HFSS to illustrate the sensitivity described above. As can be seen in Fig. 19, the ground structure is made to minimize capacitance between the windings and ground. However, such capacitance is still significant as can be seen in the data that follows. In Fig. 20 the magnitude of the ratio of Y_{12} and Y_{13} is plotted for the transformer in Fig. 19 and for the same transformer with an electrostatic shield inserted between the primary and secondary. As can be seen this ratio, which indicates the symmetry of the admittance parameters, is very nearly unity (0 dB) in both cases although the presence of the electrostatic shield degrades the ratio slightly. In Fig. 21 the phase of the ratio of Y_{12} and Y_{13} is plotted for the transformer in Fig. 19 and for the same transformer with an electrostatic shield inserted between the primary and secondary. Again, this phase is very nearly $180°$ in both cases although again the presence of the electrostatic shield perturbs it slightly from the ideal value. In Fig. 22 the magnitude of the ratio of Z_{12} and Z_{13} is plotted for the transformer in Fig. 19 and for the same transformer with an electrostatic shield inserted between the primary and secondary. The data illustrates the central point of this section. As can be seen this ratio of impedance parameters, which indicates the symmetry of the open-circuit output voltages, is approximately 14 dB for the transformer with no shield, but is only approximately 1 dB when the shield is in place. The shield has a *pronounced* effect on the symmetry of the open-circuit output voltages and hence the symmetry of the balun when operating into high-impedance loads. In Fig. 23 the phase of the ratio of Z_{12} and Z_{13} is plotted for the transformer in Fig. 19 and for the same transformer with an electrostatic shield inserted between the primary and secondary. Again, the presence of the shield forces the phase of the ratio $\frac{Z_{12}}{Z_{13}}$ closer to its ideal value of $180°$. Finally, in Fig. 24 the magnitude of the ratio $\frac{Y_{22}}{Y_{23}}$ is plotted for the transformer with and without the shield. As can be seen, the shield degrades this ratio slightly from its ideal value of 0 dB, although the effect is slight. In Fig. 25 the magnitude of

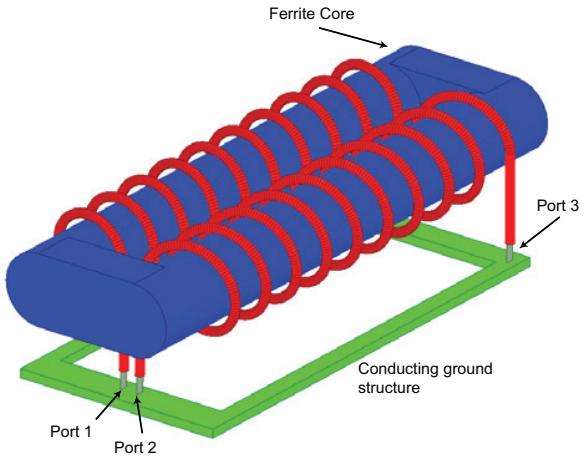

Fig. 19. Simple Faraday transformer with ferrite core. The green conductive frame at the bottom serves as a ground and the three lumped ports in the simulation can be seen connecting the red windings to ground.

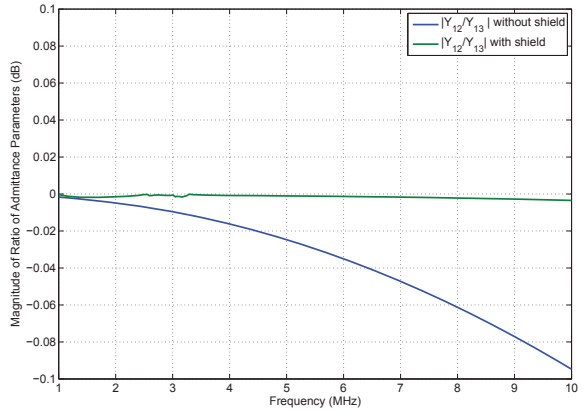

Fig. 20. The magnitude of the ratio $\frac{Y_{12}}{Y_{13}}$ with and without the electrostatic shield. Note the y-axis scale–the shield changes the magnitude of the ratio $\frac{Y_{12}}{Y_{13}}$ by less than 0.1 dB.

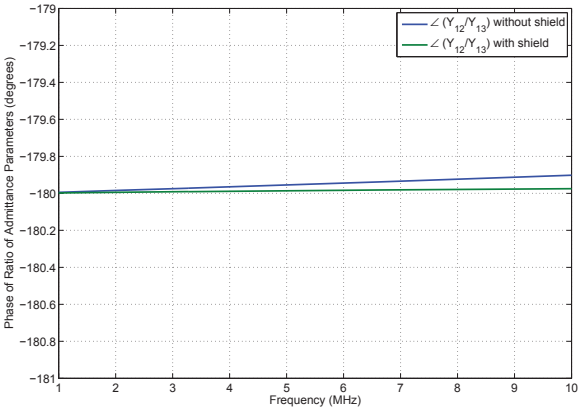

Fig. 21. The phase of the ratio $\frac{Y_{12}}{Y_{13}}$ with and without the electrostatic shield. Again note the y-axis scale–the shield changes the phase of the ratio $\frac{Y_{12}}{Y_{13}}$ by less than $0.1°$.

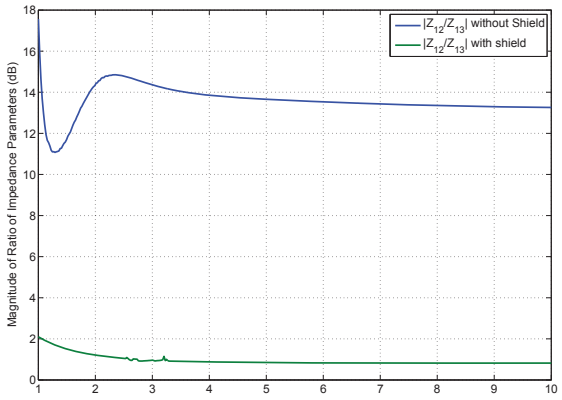

Fig. 22. The magnitude of the ratio $\frac{Z_{12}}{Z_{13}}$ with and without the shield. As can be seen, the magnitude of the ratio $\frac{Z_{12}}{Z_{13}}$ is approximately 14 dB without the shield, but is reduced to less than 1 dB with the shield. This simulated data illustrates one of main points of this paper–the shield does little to perturb the short circuit current balance, but dramatically improves open-circuit voltage balance.

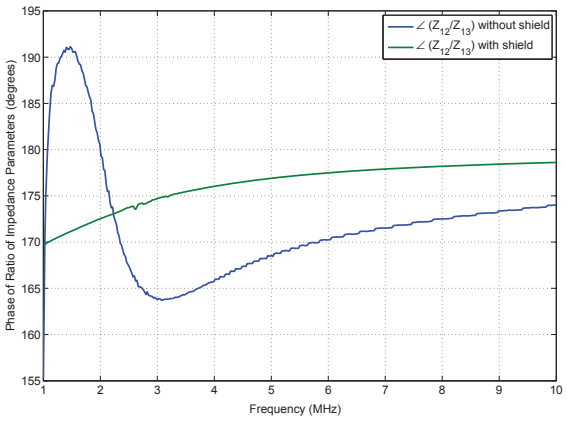

Fig. 23. The phase of the ratio $\frac{Z_{12}}{Z_{13}}$ with and without the shield. Again, the shield forces this phase much closer to its ideal value of 180°.

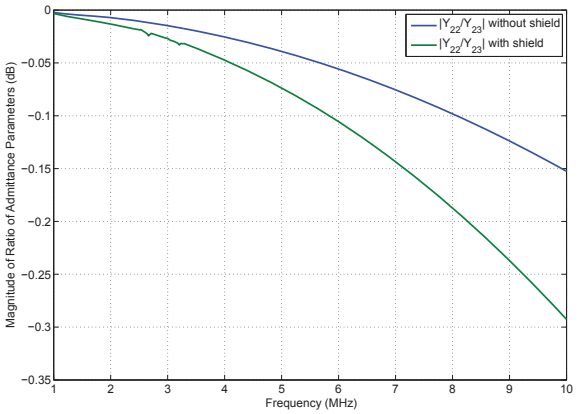

Fig. 24. The magnitude of the ratio $\frac{Y_{22}}{Y_{23}}$ with and without the shield. As can be seen, the shield does degrade the current balun behavior slightly as the ideal value of this ratio is 0 dB for a current balun. Nevertheless, the degradation is small.

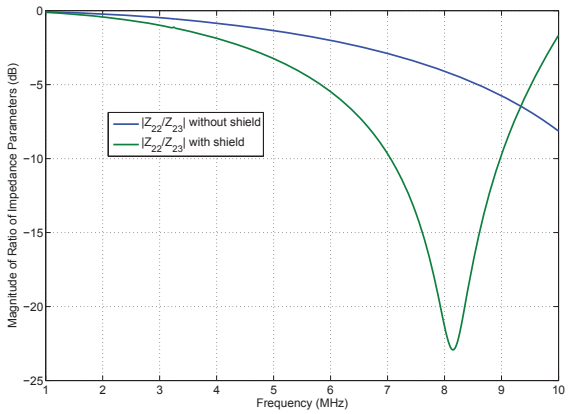

Fig. 25. The magnitude of the ratio $\frac{Z_{22}}{Z_{23}}$ with and without the shield. The behavior of the magnitude of the ratio of $\frac{Z_{22}}{Z_{23}}$ is complicated by the unavoidable presence of capacitance to ground even without the shield. Nevertheless the shield changes this ratio markedly and the transformer with a shield cannot serve as a true voltage balun.

the ratio $\frac{Z_{22}}{Z_{23}}$ is plotted for the transformer with and without the shield. As can be seen, the shield changes this ratio significantly, but this only indicates that, similarly to the balun described by Eqn. 31, the device with the shield is neither a voltage nor a current balun, but rather simply a general symmetric balun. The change in the ratio $\frac{Z_{22}}{Z_{23}}$ in Fig. 25 due to the shield is not as dramatic as would be expected from comparing Eqns. 28 and 31 because there is significant capacitance from the windings to ground even without the shield. That is, this capacitance is a significant fraction of the inter-winding capacitance. In summary, the original Faraday transformer behaved as a reasonably good current balun as can be seen in Figs. 20, 21, and 24. One might note that $Y_{22} = Y_{33}$ due to symmetry for this transformer. However, the current balun produced highly unbalanced open-circuit output voltages as shown in Figs. 22 and 23. Inserting an electrostatic shield between the primary and secondary forced the open-circuit output voltages to be fairly well balanced and only slightly degraded the ratio $\frac{Y_{12}}{Y_{13}}$ as seen in Fig. 24. However, this addition did change the ratio $\frac{Y_{22}}{Y_{23}}$ thus degrading the current balun action and therefore producing instead a symmetric balun which rigorously balances neither current nor voltage. Nevertheless, the degradation seems small.

IX. Conclusions

This paper can be summarized in four statements:

1) *Balance* as quantitatively described by Eqn. 1, implies the 3-port network in Figs. 2, 3, and 4 enforces the magnitude of a particular power conjugate variable (e.g.

voltage) to be equal at the two output ports, ports 2 and 3 while the relative phase is $180°$. This action is independent of the 3-terminal, 2-port passive load.

2) *Symmetry*, on the other hand, as quantitatively described by Eqn. 5, implies that a transposition of the two output ports, ports 2 and 3, causes exactly the same action as a $180°$ phase shift in the driving function at port 1. Perfect or ideal voltage and current baluns as well as $180°$ power dividers are symmetric. The property of symmetry is broader than balance. That is, ideal baluns are a subset of symmetric 3-port networks using the definition here.
3) If a 3-port balun exhibits *perfect* symmetry as described by Eqn. 5 for one port variable, e.g. voltage, it will exhibit symmetry for the other port variables such as current. Such an ideal network will balance short-circuit currents and open-circuit voltages, but not necessarily current or voltage in any intermediate case. Any 3-port balun satisfying the symmetry requirement given in 5 for some port variable, will exhibit similar symmetry for any linear combination of port variables. It will balance some particular port quantity such as that given in Eqn. 18 that is one of these linear combinations of port voltages and currents.
4) In a practical balun with a very slight asymmetry, for example a current balun with a slight asymmetry in the short-circuit output currents, demanding that the output coupling conform to that of an ideal current balun ($Y_{22} = Y_{33} = -Y_{23}$) results in *highly* asymmetric open-circuit output voltages.
5) An ideal $180°$ hybrid network with a general, complex terminating impedance at the sum port represents the generalized symmetric balun as described in Eqn. 5. That is, any passive termination at the sum port of the hybrid results in a symmetric 3-port balun. This result is more general than that in ref. [10].

The antenna/balun symmetry tests described in ref. [2] and ref. [3] do not prefer any particular type of balun but rather simply require the symmetry described by Eqn. 5. Of course, if a balun is not substantially symmetric, it must be rejected. However, current balance requires more than symmetry–it requires the scattering matrix in Eqn. 13 with $\Gamma = 1$ and it seems clear that current balancing is what will result in minimal CM current on the feed transmission line when the antenna is vertically polarized. Thus, the question arises as to why any other type of balun should be preferred. One reason would be that given a particular approach to implementation, e.g. transmission-line transformer, some types of baluns are more easily realized. If, for example, a voltage balun were easier to make symmetric than would be a current balun, then this type is what must be used as a current balun with poor symmetry would not be preferable over a voltage balun with nearly perfect symmetry. Ideal voltage and current baluns are limiting cases of symmetric 3-port networks and their respective, natural matrix representations, the impedance matrix of the voltage balun and the admittance matrix of the current balun, are singular and have no inverses. A current balun with a very slight short-circuit imbalance exhibits a nearly singular admittance matrix leading to a very asymmetric impedance matrix and hence can produce wildly unbalanced open-circuit output voltages. This was shown numerically and experimentally for an equal-delay impedance transforming balun in ref. [19] and was also demonstrated here with a numerical simulation of a Faraday isolation transformer with and without an electrostatic shield between the primary and secondary windings. Finally, the sensitivity of the impedance matrix symmetry of the current balun can be seen in the condition number of its admittance matrix.

REFERENCES

[1] J. S. McLean and H. Foltz, "Symmetry vs. Balance in Balancing Networks for Dipolar Antennas," in *Proc 2019 IEEE Intl. Symp. Electromagn. Compat.*, New Orleans, pp. 117-122, 22-26 July, 2019

[2] ANSI C63.5-2017: Section 4.4.3 "Antenna symmetry measurement, 30 MHz to 300 MHz," Wash. DC, 2017.

[3] CISPR 16-1-4, Section 4.5.4.2 "Balun DM/CM conversion check", Geneva, Switzerland, 2010.

[4] W. Schaefer, "Antenna Parameters and Antenna Calibration," *In Compliance Magazine*, Avail. Online: incompliancemag.com, June 30, 2016.

[5] Z. Chen and A. Adhyapak, "Limitations of symmetry test method for antennas as specified in ANSI C63.5-2006 standard," in *Proc. 2016 IEEE Intl. Symp. Electromagn. Compat.*, pp. 679-683, Ottawa, Aug. 2016.

[6] M. J. Alexander, "Measurement Good Practice Guide No. 4: Calibration and Use of EMC Antennas," National Physical Laboratory Teddington, Middlesex, United Kingdom TWll OLW, April 1997.

[7] M. J. Alexander "Antenna Measurements II: Calibration of ELF to UHF Wire Antennas, Primarily for EMC Testing," in *Microwave Measurements: 2007*, pp 459-471, IET, Stevenage, UK, pp. 2007.

[8] M. J. Alexander, "Using Antennas to Measure the Strength of Electric Fields near Equipment," *CE Magazine*, Dec. 2004.

[9] M. J. Alexander, M. H. Lopez, and M. J. Salter "Getting the Best out of Biconical Antennas for Emission Measurements and Test Site Evaluation," in *Proc. IEEE Intl. Symp. Electromagn. Compat.*, Austin, TX, Aug. 1997.

[10] J. S. McLean, "Balancing Networks for Symmetric Antennas-I: Classification and Fundamental Operation," *IEEE Trans. Electromagn. Compat.*, Vol. 44, No. 4, pp. 503-514, Nov. 2002.

[11] J. C. Willems, "Terminals and Ports," in *Proc. 2010 IEEE Intl. Symp. Circuits and Systems*, pp. 81-84 Paris, 30 May-2 June, 2010, .

[12] I. Busch-Visniac, *Electromechanical Sensors and Actuators*, Springer, New York, 1999.

[13] J. S. McLean, "Analysis of the Equal-Delay Topology for Transformers and Hybrid Networks," *IEEE Trans. Electromagnetic Compatibility*, Vol. 48, No. 3., pp. 516-521, Aug., 2006.

[14] E. F. Sartori, "Hybrid Transformers," *IEEE Trans. Parts, Materials, Packaging*, Vol. PMP-4, No. 3, pp. 59-66, Sept. 1968

[15] H. J. Carlin and A. B. Giordano, *Network Theory: An Introduction to Reciprocal and Nonreciprocal Circuits*, pp. 245-249, Prentice- Hall, Englewood Cliffs, NJ, 1964.

[16] J. S. McLean, "Rigorous Representation of a Shielded Three-Port Balun in the Simulation of an Antenna System," *IEEE Trans. Electromagn. Compat.*, Vol. 50, No. 3, Aug. 2008.

[17] H. Uchida, *Fundamentals of Coupled Lines and Multiwire Antennas*, Sasaki Printing and Publishing C, 1967.

[18] J. S. McLean, K. Takizawa, M. Midori, H. Kurihara, and R. Sutton, "The Electric Field Response of the Van Veen Loop," in *Proc. EMC Tokyo 2014*, pp. 505-508, May 2014.

[19] J. S. McLean, "The Performance of Balancing Networks Derived from the Shunt-Series, Equal-Delay Hybrid," in *Proc. IEEE 2019 Intl. Symp. Electromagn. Compat.*, New Orleans, July 22-26, 2019

[20] G. Strang, *Linear Algebra and its Applications*, 2nd Ed., Academic Press, New York, pp. 280-285, 1980.

[21] K. L. Kaiser, *Electromagnetic Compatibility Handbook*, CRC Press, pp. 17-52–17-58 Boca Raton, FL. 2005.

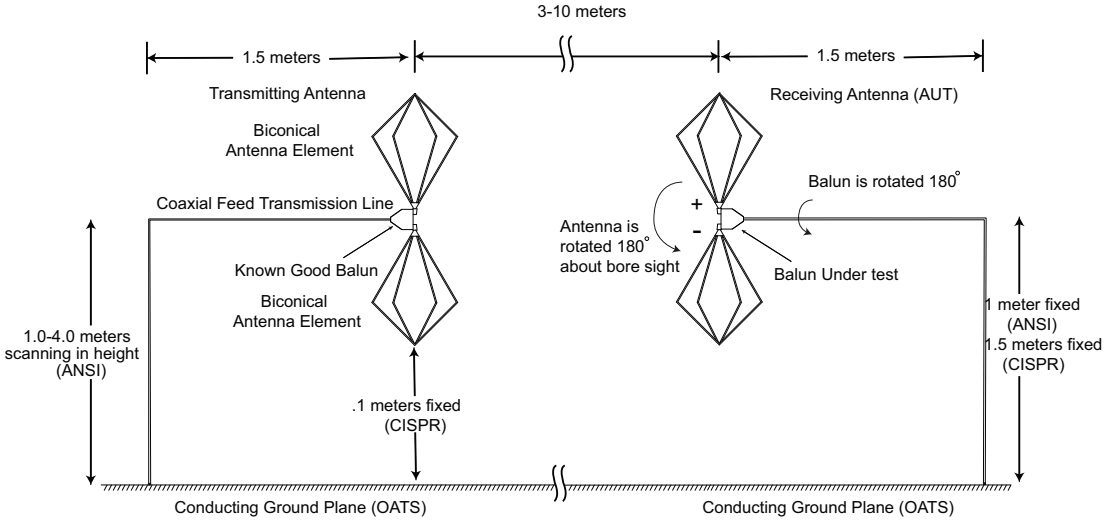

Fig. 1. Balun symmetry test: The antenna on the left is known good and is to be a source of vertically-polarized, quasi-plane wave radiation. In the ANSI standard this antenna is scanned to avoid nulls due to interference between the LOS and ground bounce rays. In some of the original NPL tests, this antenna was a monopole. The inversion is performed by rotating the balun and antenna on the right 180º about its bore-sight axis such that the minus sign is up and the plus sign down.

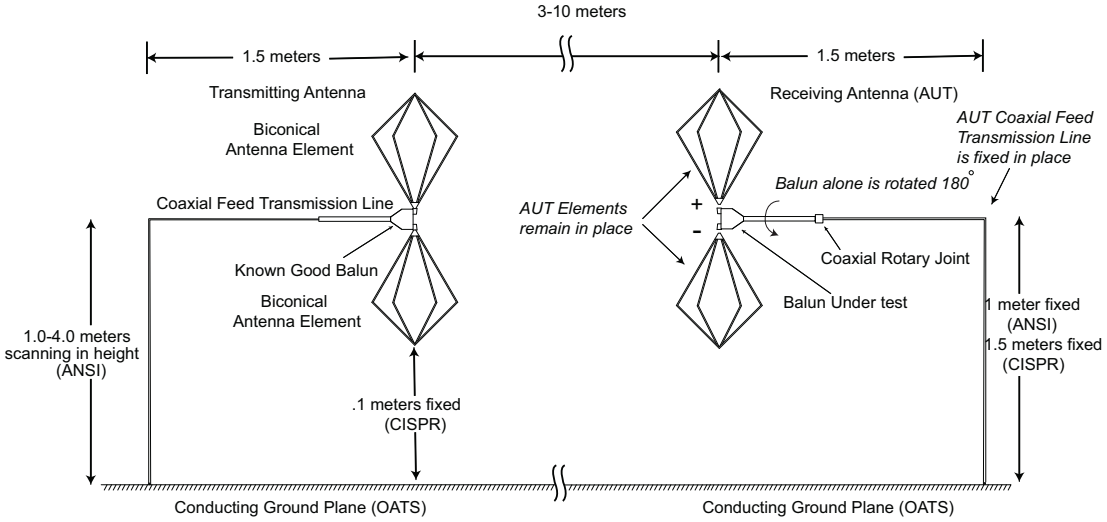

Fig. 5. Balun symmetry test thought experiment: An ideal coaxial rotary joint is connected between the AUT balun and the coaxial feed line for the AUT. The AUT feed transmission line is rigidly fixed in place. The AUT radiating elements are detachable from the balun and (somehow) held in place such that the inversion is performed by rotating only the balun on the right 180º such that the minus sign is up and the plus sign down. To rephrase this, only the AUT balun is inverted; everything else stays in place.